Formation of self-rolled polymer microtubes studied by combinatorial approach

Kamlesh Kumar [a,*], Valeriy Luchnikov [b], Bhanu Nandan [a],
Volodymyr Senkovskyy [a], Manfred Stamm [a,*]

[a] Leibniz Institute of Polymer Research Dresden, Hohe Strasse 6, 01069 Dresden, Germany
[b] Institute de Chimie des Surfaces et Interfaces, rue Jean Starcky 15, 68057 Mulhouse, France

ARTICLE INFO

ABSTRACT

This paper describes an experimental study of the polymer microtube formation in different fabrication conditions. A photolithography route is demonstrated for the fabrication of large amount of uniform and good quality polymer microtubes. TEM grids were used as mask and exposure of UV radiation was done in two steps to create asymmetric patterns. The diameter of tube was controlled by regulating the thickness of polymer layers, UV radiation dose and concentration of acidic solution. The results indicate that thickness of the bilayer film was the most dominating factor to determine the tube's dimension, and diameter of the tubes increased with increase in the thickness of bilayer. The kinetics of the tube formation was studied with respect to acidity of the solution and UV dose. Rate of rolling increased with the acidity of the solution. Tube diameter and rate of rolling decreased with the increase of the UV exposure time. Films with two-dimensional gradients of layer thicknesses were prepared to study a broad range of parameters in a single experiment. The tubes were characterized in detail using optical microscopy and scanning electron microscopy. These polymer microtubes have potential applications in microfluidic devices and biotechnology field.

1. Introduction

Polymer micro- and nanotubes have been demonstrated to possess remarkable applications in various fields such as microfluidic devices [1], chromatography [2], biotechnology [3], medicine [4] and chemical sensors [5]. Recently, a novel approach for fabrication of such mesoscopic tubes by self-rolling of strained bilayer film was developed [6–13]. A thin bilayer film minimizes its potential energy by bending and scrolling when the strained top and bottom layer is allowed to relax. Strain in this case develops due to unequal swelling of polymers in selective solvents. The rolled up layers stick together thus forming a perfectly bonded tube wall. The main advantage of self rolling technique is the possibility of complex engineering of future inner walls of the tubes [14,15]. The small dimensions and the remarkable physio-chemical properties of their inner walls are important for the micro and nanofluidic systems because ion and chemical transport can be regulated by molecular-recognition sites on the channel wall [16].

Although the general principle of the tube's formation via self-rolling is well known today, the dependence of the tube's characteristics on the dimensions of rolling bilayer and the parameters of fabrication are still poorly understood. The goal of our present paper is experimental systematic study of the polymer microtube formation in various fabrication conditions. We explore the dependence of the tube's diameters on the thickness of each of the polymer layers in the double-layer structure. Then, the dependence of the tube's diameters on the degree of short-wavelength UV cross-linking is investigated.

* Corresponding authors. Fax: +49 3514658281.
   E-mail addresses: kumar@ipfdd.de (K. Kumar), stamm@ipfdd.de (M. Stamm).

Finally, the rate of rolling as a function of the UV exposure dose and solvent selectivity are obtained. Also, in the present paper we report the improvements in the photolithography route to microtube fabrication, which permits parallel production of large amount of uniform, high quality tubes.

2. Fabrication scheme

Poly(4-vinylpyridine) (P4VP) {M_n = 45,900, M_w = 82, 500} and Polystyrene-b-Poly(4-vinylpyridine) (PS-b-P4VP) {M_n = 35,000−2700} were obtained from Polymer Source Inc. Poly(4-bromostyrene) (BrPS) was synthesized from 4-bromostyrene by nitroxide mediated radical polymerization. Ten grams of freshly distilled 4-bromostyrene (0.055 mol) and 0.032 g of 2,2,5-Trimethyl-3-(1-phenylethoxy)-4-phenyl-3-azahexane, alkoxyamine (0.1 mmol) were placed in a round bottom flask equipped with magnetic stirring bar and sealed with a rubber septum. Argon was bubbled through the mixture using stainless steel needle for 30 min. After that the mixture was heated at 123 °C for 2 h. The viscous polymer solution so obtained was diluted with tetrahydrofuran (THF) and poured into hexane. The solid was filtered, redissolved in dichloromethane and precipitated into tenfold excess of diethyl ether and dried in vacuum at 50 °C. Yield – 8 g (80%). GPC: M_n = 25, 000, M_w = 46,000, PDI = 1.77}. 4-Bromostyrene was purchased from Sigma–Aldrich and distilled under reduced pressure before use. THF, diethyl ether and hexane were purchased from Sigma–Aldrich. Toluene, chloroform and dichloromethane were purchased from Acros Organic and used as received.

Silicon wafer were used as the substrates and were cleaned before their use by sonication in dichloromethane for 15 min followed by heating in H_2O_2, NH_4OH and milipore water solution (1:1:2) for 1 h at 65 °C. Subsequently the silicon wafers were rinsed 3–4 times with millipore water and dried under nitrogen stream. A polymer bilayer was created by consecutive deposition of P4VP and BrPS, from chloroform and toluene solutions, respectively, by dip-coating technique. A 4–5 nm thin layer of PS-b-P4VP block copolymer was deposited on the P4VP layer before deposition of BrPS, in order to provide a better adhesion between the BrPS and P4VP layers. Photolithography was used for patterning the bilayer. UV lamp (G8T5, TecWest Inc., USA) having a 2.5 W output at 254 nm was used to irradiate the P4VP/BrPS bilayer. The estimated exposure dose was 4.11 J/cm² for 30 min. Irradiation with <280 nm UV light is known to lead to generation of free radicals, chain scission and crosslinking of PS [17] and P4VP [18]. TEM copper grids (400 lines per inch) were used as a photo mask. Irradiation with short-wave UV (λ = 254 nm) causes photo-crosslinking of BrPS and P4VP in irradiated regions. The pattern was developed by washing the uncured polymer (both BrPS and P4VP) using a non-selective solvent (chloroform). Finally, the microtubes were produced by immersion of the samples in aqueous solutions of hydrochloric acid (HCl). The protonation of pyridine rings results in Columbic repulsion of the 4VP units and selective swelling of the P4VP layer. This swelling, opposed by the stiff BrPS layer, gives rise to the bending moment in the film,

that leads to the film detachment from the substrate and curling (Fig. 1). Since the BrPS layer acts as the protective layer for the P4VP one, the rolling starts and proceeds from the opening in the film, produced by photo-patterning. More detailed description of the photolithography route is described elsewhere [14].

Self-rolling from uniform openings in the bilayer, produced either by photolithography or any other approach (e.g. mechanical scratching) results usually in twin tubes [10,19]. In order to obtain the uniform single tubes, we apply the procedure of asymmetric photo-patterning (Fig. 2). The polymer bilayer is exposed twice to the UV light, once at the normal incident angle, and then at a certain inclination. After the development of the pattern in chloroform, the asymmetric ratchet-like profile of the bilayer is obtained (Fig. 2d). The tubes are formed by rolling from the steeper edges of the polymer stripe. This is so because the adhesion energy does not depend on the thickness of the film, although the bending energy does. At the thin side of the profile, the gain of energy via rolling is insufficient to prevail the adhesion to the substrate, whereas at the steep side the bending moment is strong enough to detach the film from the surface.

Optical micrographs of polymer bilayers with typical developed patterns and their unidirectional rolling are shown in Fig. 3a and b. Optical micrograph of twin tubes and SEM micrograph of tubes are shown in Fig. 3c and d, respectively.

3. Effect of fabrication parameters on the diameter of tubes

The diameter of the tubes depends on a number of factors, the most important being the thickness of each of the components of the bilayer, the stiffness of the polymer networks in the collapsed and the swollen states, the degree of swelling, and the strength of adhesion to the substrate. In the present study, we do not attempt to make a more detailed comparison of the experimental data with a theoretical model. This comparison is not possible at the present state of our knowledge about the system for several reasons. First, such parameters entering in the model as Young moduli of the polymers in the glassy and swollen states are not
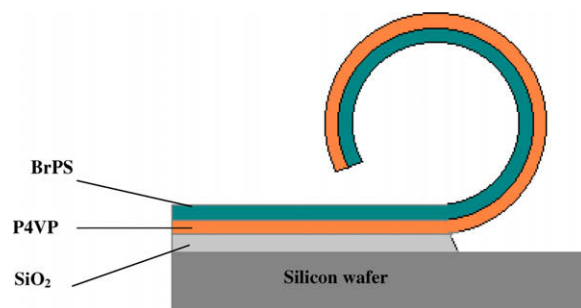

Fig. 1. Schematic presentation of self rolling of P4VP/BrPS bilayers. Rolling occurs due to etching of SiO_2 layer by the hydrochloric acid which releases the polymer film.
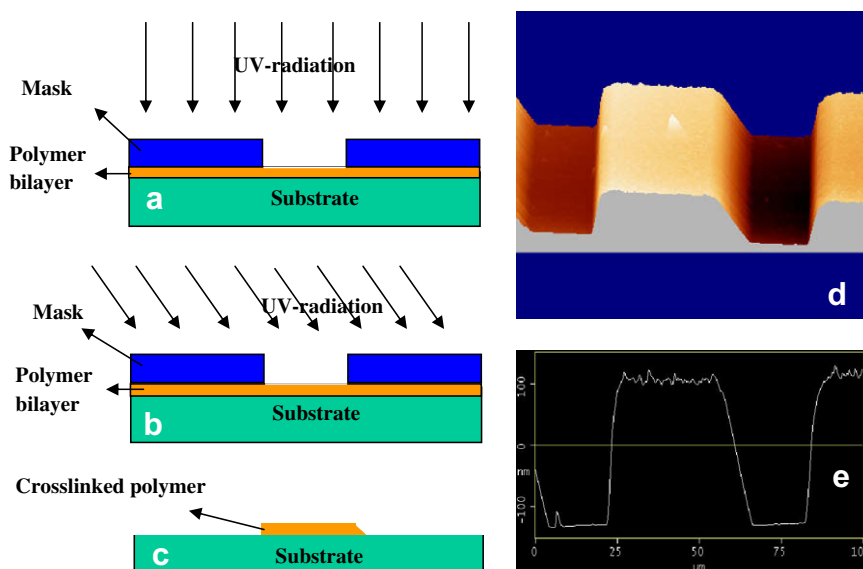
Fig. 2. The photolithography process and schematic way of formation of asymmetric pattern (a–c). (a) Sample exposed to UV light at normal incident angle, (b) sample exposed to UV light at sharp incident angle, and (c) development of pattern after washing away uncrosslinked polymer. (d) Three-dimensional AFM image of an asymmetric polymer stripes, and (e) section profile of AFM image.
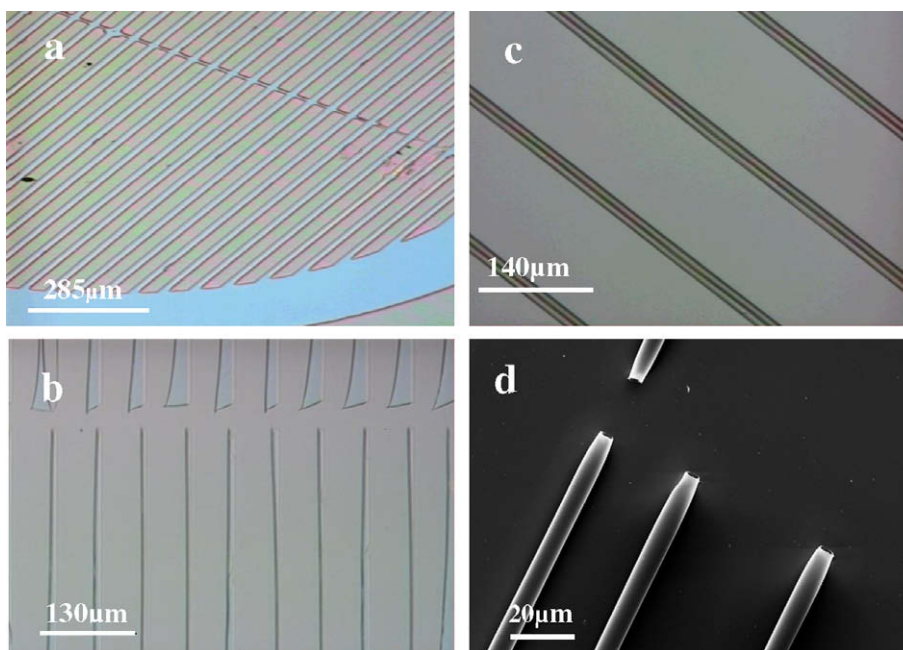

Fig. 3. Tube formation by self rolling of photo-structured bilayer film. (a) Pattern developed by washing away uncrosslinked polymer with chloroform. (b) Unidirectional rolling of asymmetric polymer stripe in 0.1 wt% aqueous solution of HCl. (c) Formation of twin tube from the symmetric polymer stripe. (d) SEM micrograph of arrays of tubes.

known and their measurement in the bilayer film needs the development of special techniques. Second, the Timoshenko formula, derived for the limiting case of linear elasticity theory of the materials, may not be adequate for the description of the polymer bilayer films. Such effects like yielding of the glassy polymer layers upon elongation, and non-linear stress–strain relation of the polymer networks upon strong elongation should be taken into account. For this reason, we constrain the goal of the present paper to tracing the main tendencies of the tube's formation process, with the purpose to elaborate the practical recommendation for the microtube fabrication procedures, and with the aim to provide the material for future theoretical analysis.

3.1. Dependence of the tube's dimensions on the thickness of the polymer layer

Thickness of the BrPS and the P4VP layers are the characteristics of the bilayer that can be most easily controlled during the fabrication process. Dip-coating technique permits to control the thickness of the polymer layer simply by varying the rate at which the sample is withdrawn from the solution. According to the model of Landau and Levich, the effect of the solution viscosity on the film thickness (h) is as significant as the effect of the withdrawal speed (u_{o}), which can be described by $h \propto (u_{o})^{0.67}$ [20]. Remarkably, the dip-coating technique also allows easy creation of samples with a gradient of the film thickness along the sample length, via accelerating (or decelerating) the rate of the sample withdrawal from the solution. This enables to explore the tube's formation for a continuum of the layer thickness values in a single experiment. This so-called combinatorial approach is nowadays broadly used in chemistry and material science [21]. In order to simplify the study of the bilayer films, we create samples with 2D-film thickness gradients. First, the P4VP layer is deposited so that its thickness increases from top to bottom along the conventional X direction. The thickness of the layer is measured at several points along the X direction and linearly interpolated that gives the thickness of the layer as the function $g(X)$. Then, the sample is rotated by 90° and the BrPS layer is deposited with the thickness gradient along the conventional Y-axis. The thickness of the bilayer is again measured by ellipsometry, this time along the Y direction, and the thickness of the BrPS layer is interpolated by the function $f(Y)$ (the thickness of the P4VP layer is deduced). Then, the thickness of the bilayer film at any point of the sample can be calculated as $h(X,Y) = g(X) + f(Y)$. For future reference, we present in Fig. 4 the dependences of the BrPS and P4VP film thickness on the rate of dip-coating, for different solution concentrations. A photo-patterned sample with the 2D-gradient of the bilayer thickness is shown on Fig. 5.

The tubes were formed by immersion of the patterned bilayer in the 0.1 w.t.% aqueous HCl solution. In the present work, we omit the study of the dependence of the tube's diameters on the solvent quality. The HCl concentration chosen by us is optimal in the sense that it is not only sufficiently high for the initiation and proceeding of the rolling, but it is also sufficiently low to avoid very rapid scrolling, that usually leads to defects and irregularities of the tube shapes. With the dip-coating technique, we were able to generate gradient films with the thickness increasing approximately by 100% along the sample, both for BrPS and P4VP layers. There exists a minimal thickness of the P4VP layer (approximately 35 nm) that is required to provide the bilayer films sufficient bending moment, necessary to overcome the adhesion to the substrate.

Fig. 6 shows the dependence of the tube's diameters on the thickness of the BrPS layer (before swelling) for several thicknesses of the P4VP layer. Samples were irradiated with 8.22 J/cm² UV dose. In our experimental conditions the diameter of the tube grows with the thickness increase of either of the layers. It is clear however from general considerations that the radius of the curled film should have a
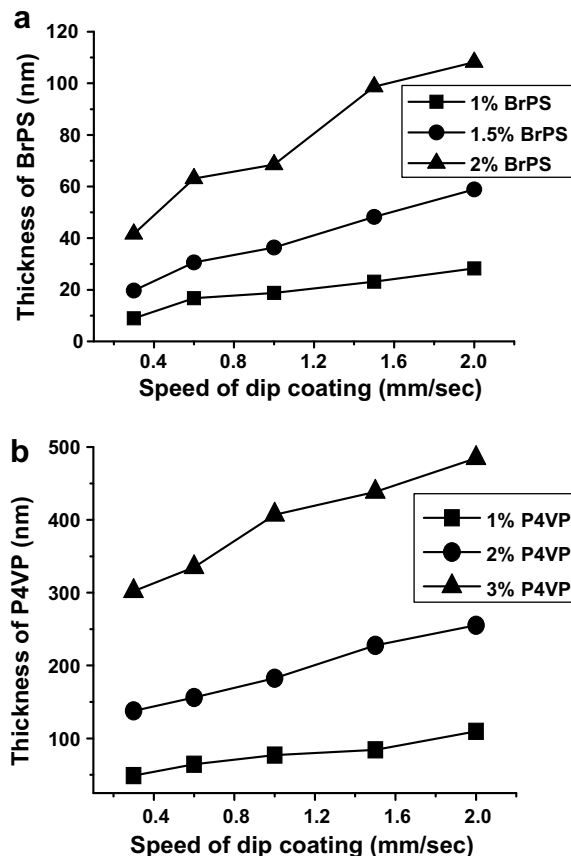

Fig. 4. The dependence of film thickness on P4VP and BrPS solution concentration and speed of dip coating. (a) Thickness of BrPS vs speed of dip coating from solution in toluene. (b) Thickness of P4VP vs speed of dip coating from chloroform.
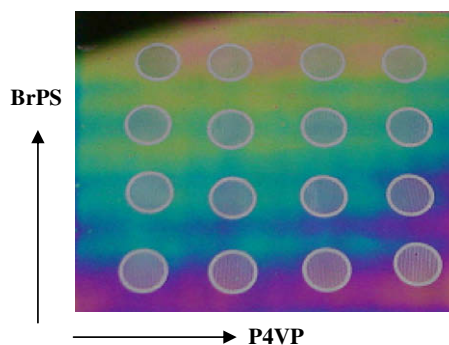

Fig. 5. The BrPS/P4VP photo-patterned film with gradient thickness. TEM grids were used as a mask to create pattern. On the image, the thickness of BrPS and P4VP increases along the vertical and horizontal directions, respectively. The arrows show the direction of increasing thickness of BrPS and P4VP.

minimal value for a certain optimal ratio of the layer thicknesses, for any fixed total thickness of the bilayer. If, for example, the bottom layer is very thin in comparison to the top layer, its expansion is not able to generate a strong bending moment, and the curvature radius aspires to infinity. If, in contrary, the bottom layer is very thick, its
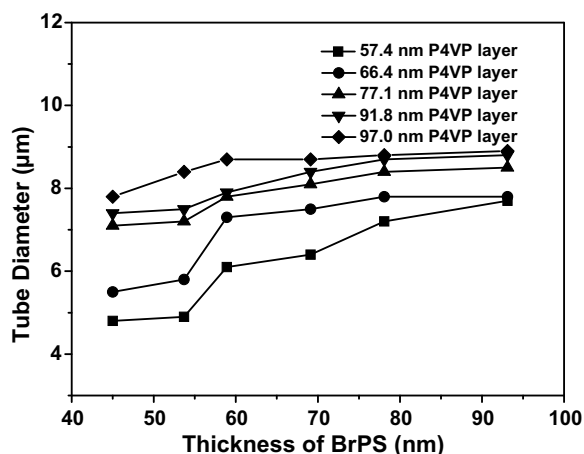
Fig. 6. Dependence of the diameter of tubes at different thickness of P4VP and BrPS.

expansion cannot be effectively constrained by the counter-force arising in the top layer, that also results in a big radius of the curl. In Appendix A, we show the theoretical dependence of the bilayer curvature layer thicknesses calculated according to the Timoshenko formula [22]. This probably means that in the experiment we are able to scan only a restricted region of parameters, marked by an arrow on Fig. A.1.

3.2. Effect of UV exposure dose on tube diameter

Bilayer film with BrPS and P4VP of thickness 50 and 90 nm, respectively, were used to study the effect of UV exposure dose and concentration of acidic solution on tube diameter and rate of rolling. Samples were exposed to UV radiation for different time to study the effect of UV exposure dose. Patterned samples were put in 0.1 wt% aqueous solution of HCl for rolling. The dependence of the tube diameters on the UV exposure dose is shown in Fig. 7. It is observed that only the films exposed to the minimum
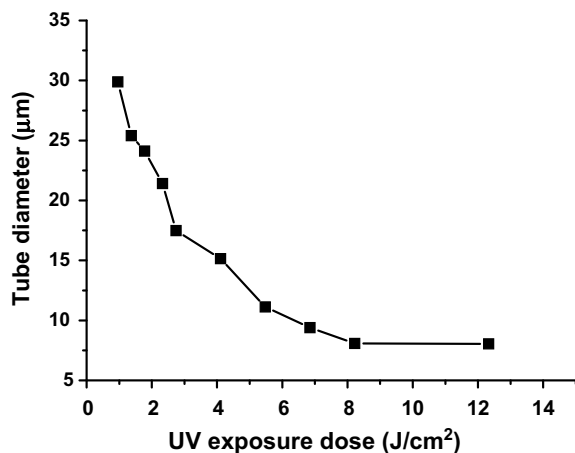
irradiation dose 0.96 J/cm^2 are able to roll in the acidic solution. The experiment shows that tube diameter continuously decreases with increasing the exposure time, until the radius of the tubes reaches some saturation value, after which no further change was observed. Possibly, this saturation value is determined by the limiting degree of cross-linking, determined by the micro-structure of the polymer. In a future study, the dependence of the tube's diameter on the irradiation dose will be analysed in more details.

3.3. Rate of rolling for different UV irradiation doses

UV irradiation affects not only the geometrical dimensions of the tubes, but also the rate of the tube's formation, as shown in the Fig. 8. The rolling tubes were video-recorded and the rate of their formation was determined as the distance passed by a tube's axis in the time unit.

There can be two reasons for the deceleration of the tube's formation with the increasing UV dose. Higher crosslinking degree may slow down the mobility of polymer chains and the rate of swelling of the P4VP network in the solvent. It is also known that UV irradiation may cause covalent binding of polymers to SiO$_2$ substrates [23]. Then, the rolling at higher irradiation doses may be decelerated by more dense chemical links between the layer and the substrate.

3.4. Rate of rolling and the diameter of the tubes at different concentration of the acidic solution

The rate of rolling of the tubes can be controlled in broad limits by the concentration of acid in the water solution (Fig. 9). There exists the minimal concentration, below which the tube's rolling was not observed.

Apparently, the rate and the degree of P4VP layer protonation depends strongly on the pH of the solution. While the rate of protonation affects mainly the rate of the tube's formation, the degree of the protonation determines also the tube's dimensions, for the given degree of the P4VP cross-linking. It is worth to note that lower rates of rolling result usually in more perfect tubes, because swelling of the P4VP layer pro-
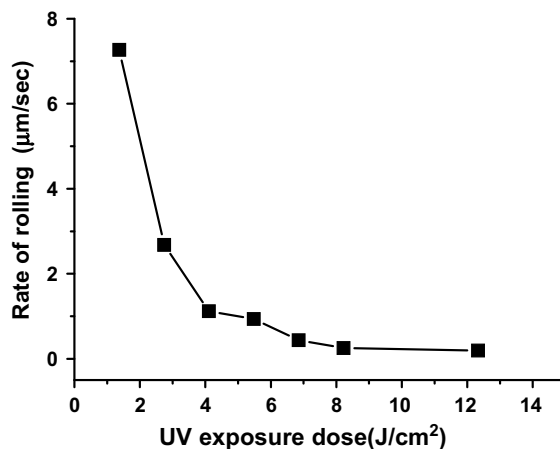

Fig. 7. Dependence of tube diameter on dose of UV exposure.

Fig. 8. Rate of rolling in 0.1 wt% HCl: rate of rolling vs UV exposure dose.
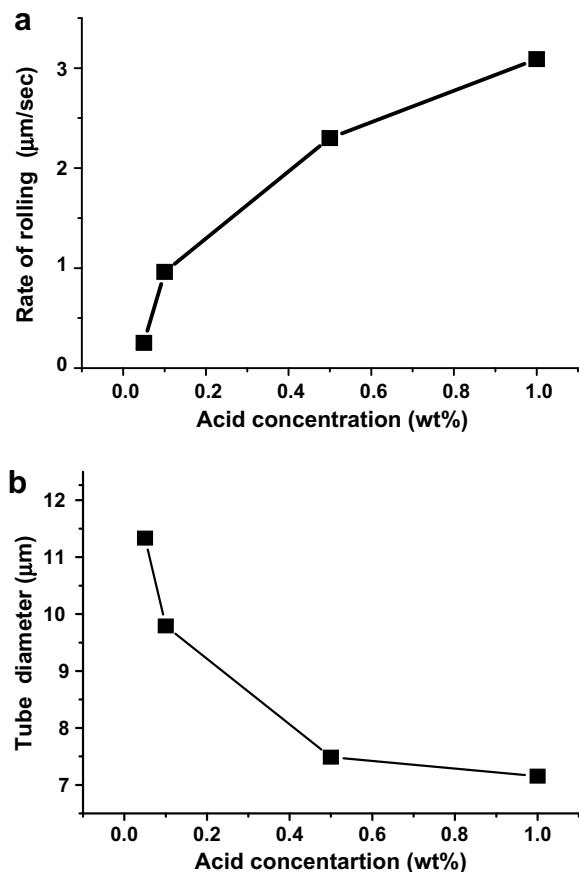
Fig. 9. (a) The rate of rolling at different acid concentration. (b) The dependence of the tube's diameter on the acid concentration. Irradiation dose is 5.48 J/cm².

ceeds more homogeneously, and defects, which have some extra free energy cost, have more time to be relaxed.

4. Conclusion

Photolithography route allows the formation of polymer rolled-up tubes in good quantity and of good quality. Asymmetric photo-patterning permits to program the direction of rolling of bilayer films and was found to be suitable for producing single tubes instead of twin tubes. In this paper, we presented the first systematic experimental study of the formation of polymer tubes. Combinatorial approach (preparation of films with 2D gradient of the film thickness) was applied to study a broad range of parameters in a single experiment. The dependence of the tube's dimensions on the characteristics of the bilayer films and fabrication parameters such as effect of UV radiation exposure time and effect of acid concentration on the rate of rolling are analysed. The main results can be summarized as follows: (a) thickness of the bilayer film was found to be the dominating factor to determine the tube's diameters, (b) diameter of the tubes decreased with increase in the UV irradiation dose applied for the crosslinking of the polymer, and (c) the rate of rolling and the diameter of the tubes can be effectively controlled both by the dose of the UV irradiation and the quality of the solvent (i.e. in the given system, the acidity of the water solution). However, in this paper, we constrained ourselves to qualitative explanations of the observed dependencies, because many of the process parameters yet need to be experimentally determined. A quantitative explanation based on measurement of elasticity moduli of polymer film in normal and in swollen state using AFM of the self-rolling process could be interesting and will be explored in our future works. The self-rolled microtubes discussed in this article may find potential applications in microfluidic devices, biotechnology, as a sensor and in chromatography field.

Acknowledgement

Appendix A

Timoshenko formula for calculation of the radius of curvature ρ of a bilayer film (Fig. A.1), consisting of two layers with thicknesses h_1, h_2, Young moduli E_1, E_2 and coefficients of expansion α_1, α_2:

$$\rho = 6 \frac{h_1 + h_2 3(1 + m)^2 + (1 + mn)\left(m^2 + [mn]^{-1}\right)}{\alpha_2 - \alpha_1(1 + m)^2}$$
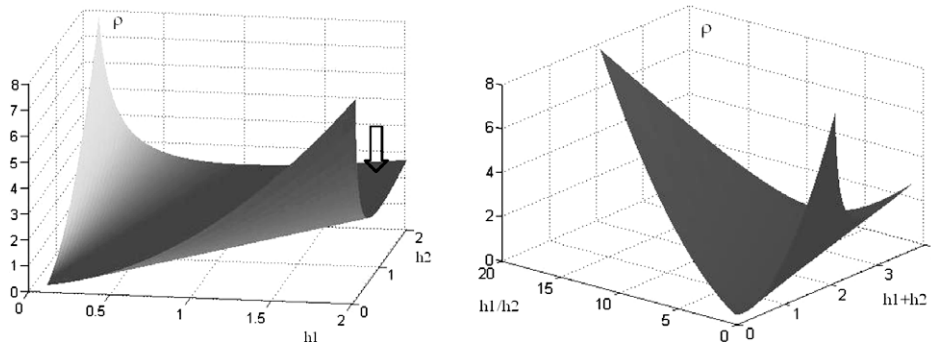
where $m = h_1/h_2$, $n = E_1/E_2$.

Fig. A.1. Radius of curvature of the bilayer (in arbitrary units) calculated according the Timoshenko formula, for $n = 1$. The arrow on the left image shows schematically the region of parameters corresponding to the experiment (see the main text).

References

[1] Sharma S, Buchholz K, Luber SM, Rant U, Tornow M, Abstreiter G. J Microelectromech Syst 2006;15(2):308–13.

[2] Ebara M, Hoffman JM, Hoffman AS, Stayton PS. Lab Chip 2006;6:843–8.

[3] Martin CR, Kohli P. Nat Rev Drug Discov 2003;2:29–37.

[4] Mcallister DV, Wang PM, Davis SP, Park JH, Canatella PJ, Allen MG, et al. Proc Natl Acad Sci USA 2003;100:13755–60.

[5] Bradley K, Gabriel JP, Star A, Grüner G. Appl Phys Lett 2003;83:3821–3.

[6] Prinz VYa, Seleznev VA, Gutakovsky AK, Chehovskiy AV, Preobrazhenskii VV, Putyato MA, et al. Physica E 2000;6:828–31.

[7] Cavallo F, Songmuang R, Ulrich C, Schmidt OG. Appl Phys Lett 2007;90:193120–3.

[8] Deneke Ch, Jin-Phillipp NY, Loa I, Schmidt OG. Appl Phys Lett 2004;84:4475–7.

[9] Prinz VYa, Chehovskiy AV, Preobrazenskii VV, Semyagin BR, Gutakovsky AK. Nanotechnology 2002;13:231–3.

[10] Luchnikov V, Sydorenko O, Stamm M. Advanced Materails 2005;17:1177–82.

[11] Golod SV, Prinz VYa, Mashanov VI, Gutakovsky AK. Semicond Sci Technol 2001;16(3):181–5.

[12] Vorob'ev AB, Prinz VYa. Semicond Sci Technol 2002;17(6):614–6.

[13] Prinz AV, Prinz VYa, Seleznev VA. Microelect Eng 2003:67–8. 782–8.

[14] Luchnikov V, Stamm M. Physica E 2006;37(1-2):236–40.

[15] Huang M, Boone C, Roberts M, Savage DE, Lagally MG, Shaji N, et al. Adv Mater 2005;17:2860–4.

[16] Huber DL, Manginell RP, Samara MA, Kim BI, Bunker BC. Science 2003;301:352–4.

[17] Ranby R, Rabek JF. Photogegradation photo-oxidation and photostabilization of polymers. New York: Wiley; 1975. p. 167–72.

[18] Harnish B, Robinson JT, Pei Z, Ramström O, Yan M. Chem Mater 2005;17:4092–6.

[19] Schmidt OG, Deneke Ch, Kiravittaya S, Songmuang R, Heidemeyer H, Nakamura Y, et al. J Select Topics Quant Electron 2002;8(5):1025–34.

[20] Thess A, Boos W. Phys Fluids 1999;11(12):3852–5.

[21] Itaka K, Yamashiro M, Yamaguchi J, Yaginuma S, Haemori M, Koinuma H. Appl Surf Sci 2006;252(7):2562–7.

[22] Timoshenko SP. J Opt Soc Am 1925;11:233–55.

[23] Yan M, Harnish B. Adv Mater 2003;15(3):244–8.